

pubs.acs.org/Biomac Article

Biodegradable Elastomers Enabling Thermoprocessing Below 100 °C

Sudipta Panja, Allison Siehr, Anasuya Sahoo, Ronald A. Siegel, and Wei Shen*



ACCESS III Metrics & More Article Recommendations Supporting Information Poly(caprolactone)-co-Poly(β-methyl-δ-valerolactone)-co-Poly(caprolactone) Semicrystalline:T... <60 °C Elastomeric Cytocompatible Low temperature processable Lysozyme Polymer Lysozyme is encapsulated 60 °C 1. Extrude in the polymer; 2. Hot Press no bioactivity is Polymer film

ABSTRACT: Biodegradable and biocompatible elastomers are highly desirable for many biomedical applications. Here, we report synthesis and characterization of poly(ε -caprolactone)-co-poly(β -methyl- δ -valerolactone)-co-poly(ε -caprolactone) (PCL-P β M δ VL-PCL) elastomers. These materials have strain to failure values greater than 1000%. Tensile set measurements according to an ASTM standard revealed a 98.24% strain recovery 10 min after the force was removed and complete strain recovery 40 min after the force was removed. The P β M δ VL midblock is amorphous with a glass-transition temperature of -51 °C, and PCL end blocks are semicrystalline and have a melting temperature in the range of 52–55 °C. Due to their thermoplastic nature and the low melting temperature, these elastomers can be readily processed by printing, extrusion, or hot-pressing at 60 °C. Lysozyme, a model bioactive agent, was incorporated into a PCL-P β M δ VL-PCL elastomer through melt blending in an extruder, and the blend was further hot-pressed into films; both processing steps were performed at 60 °C. No loss of lysozyme bioactivity was observed. PCL-P β M δ VL-PCL elastomers are as cytocompatible as tissue culture polystyrene in supporting cell viability and cell growth, and they are degradable in aqueous environments through hydrolysis. The degradable, cytocompatible, elastomeric, and thermoplastic properties of PCL-P β M δ VL-PCL polymers collectively render them potentially valuable for many applications in the biomedical field, such as medical devices and tissue engineering scaffolds.

■ INTRODUCTION

Biomaterials have broad applications in the medical field, such as implantable medical devices, drug delivery patches, tissue engineering scaffolds, and biointegrated electronics. Biodegradable, elastomeric, and biocompatible materials are highly desirable for many of these applications. Elastomeric properties are particularly important when an implant interfaces with a tissue or organ exposed to large, dynamic strains, as a mismatch in mechanical properties of an implant and adjacent tissue is known to exacerbate inflammatory responses and possibly lead to implant failure. Biodegradability allows elimination of implants after they have fulfilled their intended functions without the need for a secondary surgery, preventing potential adverse events associated with permanent implants, such as infection. ^{2,8}

Polylactide (PLA), poly(glycolic acid) (PGA), their copolymer poly(lactide-co-glycolide) (PLGA), and polycaprolactone (PCL) are biodegradable and implantable, and have

been used in many FDA-approved biomedical devices. ^{8,9} However, these materials are nonelastomeric, having small yield strains and strain to failure values. Poly(glycerolsebacate) (PGS)⁴ and poly(citrate) (PC)¹⁰ are the two most widely reported elastomers that are biodegradable and biocompatible. However, both PGS and PC are thermosets, and their synthesis involves a polycondensation step followed by curing through the reaction between carboxyl and hydroxyl groups, which is typically conducted at a temperature above 100 °C under vacuum for an extended period of time (days).^{4,10–13} The thermosetting nature and the harsh

Received: September 12, 2021 Revised: November 1, 2021 Published: December 13, 2021





synthesis conditions impose limitations on material processing and make it challenging to incorporate bioactive agents that may be necessary for some applications, such as tissue engineering scaffolds and implants for sustained delivery of bioactive molecules. Another reported biodegradable elastomer, poly(1,3-trimethylene carbonate) (PTMC), is also a thermoset polymer and requires covalent crosslinking of polymer chains dissolved in an organic solvent, making it challenging to incorporate bioactive agents as well. 17,18

Protein-based biodegradable elastomers have also been reported. Covalently crosslinked elastin (animal-derived soluble elastin or recombinant human tropoelastin) or elastin-like polypeptides exhibit elastomeric properties at physiological temperatures. ^{19–22} These materials are thermosets and therefore also have limitations in material processing as compared with thermoplastic materials. In addition, protein-based materials are costly to produce at large scales and generally raise concerns of immunogenicity when used as implantable materials. ^{19,22}

Thermoplastic and biodegradable elastomers have also been reported. Segmented polyurethanes (PUs) containing both hard pseudocrystalline domains (serving as physical crosslinks) and soft amorphous domains that have glass-transition temperatures below room temperature exhibit elastomeric properties at physiological temperature.¹⁷ These PUs can be designed to be biodegradable using various polyester-based polyols.²³ The major limitation of thermoplastic PU elastomers is that they exhibit relatively large permanent deformations and therefore do not perform well in dynamic environments. 17,24 Some polyhydroxyalkanoate-based thermoplastic polymers (PHAs), such as those synthesized through copolymerization of 3-hydroxybutyrate with either 4-hydroxybutyrate or 3hydroxybutyrate-hydroxyvalerate, are highly stretchable with large breaking strains. 25,26 However, these highly stretchable PHAs have Young's moduli on the order of GPa; even the softest material has Young's modulus greater than 50 MPa, which is much stiffer than soft tissues (the highest modulus of soft tissue is approximately 20 MPa).¹⁷ It has also been reported that random copolymerization of caprolactone with either lactide or glycolide yields elastomeric materials.^{27–30} However, random copolymerization results in poor control of molecular structure and molar mass.³¹ Polyurethane chemistry has been used to extend the chain of poly(lactide-cocaprolactone) to form multiblock copolymers exhibiting elastomeric properties. ^{14,32} However, these multiblock thermoplastic elastomers exhibit high Young's modulus (>30 MPa) and are stiffer than soft tissues.3

Biodegradable and thermoplastic PLA-co-poly(β -methyl- δ -valerolactone)-co-PLA (PLA-P β M δ VL-PLA) triblock polyesters have been reported to exhibit excellent elastomeric properties due to the amorphous midblock, P β M δ VL, having a low glass-transition temperature (-51 °C). The thermoplastic nature of these elastomers offers advantages in material processing over thermosetting elastomers. These materials are synthesized through ring-opening polymerization (ROP), allowing molecular structures and material properties to be well controlled and readily tuned. However, the processing of PLA-P β M δ VL-PLA requires a temperature of 180 °C, making it difficult to incorporate temperature-sensitive bioactive molecules.

The high processing temperature required for PLA-P β M δ VL-PLA is due to the high melting temperature of semicrystalline PLA end blocks. It was expected that triblock

polymers having P β M δ VL midblock and poly(ε -caprolactone) (PCL) end blocks would have elastomeric properties and would allow material processing at the melting temperature of PCL, which is approximately 60 °C. ^{34,35} Here, we report synthesis, characterization, and processing of triblock poly(ε -caprolactone)-co-poly(β -methyl- δ -valerolactone)-co-poly(ε -caprolactone) (PCL-P β M δ VL-PCL) polymers having various molecular compositions. We have examined mechanical properties, degradation, and cytocompatibility of these materials and shown that these thermoplastic materials are elastomeric, hydrolyzable, and cytocompatible. We have demonstrated that they can be readily processed at 60 °C through printing, extrusion, or hot-pressing, and lysozyme, a model bioactive agent, can be incorporated during material processing without losing its bioactivity.

EXPERIMENTAL SECTION

Materials. Copper chromite (Cu₂Cr₂O₅), phosphorus pentoxide (P₂O₅), calcium hydride (CaH₂), ε-caprolactone, poly(ε-caprolactone) (PCL₄₅; M_n = 45 kDa), 1,4-benzenedimethanol (BDM), diphenyl phosphate (DPP), tin(II) 2-ethylhexanoate (Sn(Oct)₂), dichloromethane (DCM), methanol (MeOH), tetrahydrofuran (THF), anhydrous toluene, lipase (from Thermomyces lanuginosus solution, activity ≥100 000 U/g), and lysozyme (activity 22 000 U/mg) were purchased from Sigma-Aldrich. 3-Methyl-1,5-pentanediol was purchased from TCI America. Fetal bovine serum (FBS), penicillin−streptomycin (10 000 U/mL), and the lysozyme activity assay kit were purchased from Thermo Fisher Scientific. Alamar Blue was purchased from Bio-Rad. Live−dead assay reagents (ethidium homodimer III and calcein AM) were purchased from Biotium.

Synthesis of β -Methyl- δ -valerolactone (β M δ VL) and Poly(β methyl-δ-valerolactone) (P β M δ VL). The cyclic β -methyl- δ -valerolactone (β M δ VL) monomer was synthesized from 3-methyl-1,5pentanediol using a previously reported procedure.³⁶ In brief, 500 mL of 3-methyl-1,5-pentanediol and 10 g of copper chromite were placed in a two-neck round bottom flask, with one neck connected to a Dean Stark trap, which was further connected to a condenser and a bubbler, and the other neck fitted with a thermometer adapter. The temperature of the flask was maintained at 210 °C by a heating mantle. Hydrogen gas produced by the reaction was allowed to pass through the bubbler. The reaction was continued overnight and stopped when no bubbling of H2 gas was observed. The monomer β M δ VL was purified from the reaction mixture through fractional distillation under reduced pressure, and the resulting product was heated over P2O5 at 120 °C for 12 h and distilled again. To further purify $\beta M\delta VL$, it was dried over CaH₂ and then distilled, and this drying and distillation procedure was completed twice. The final β M δ VL product was stored in an air-free flask until further use. The synthesis yield was ~72%. The product was characterized by ¹H and ¹³C NMR spectroscopy. ¹H NMR chemical shifts: (400 MHz, CDCl₃, 25 °C) δ 4.23 and 4.08 (-C \underline{H}_2 -O), 2.44 (-C \underline{H}_2 -CO), 1.94 and 1.74 ($-C\underline{H}_2-CH_2O-$), 1.34 ($-C\underline{H}(CH_3)CH_2-$), and 0.84 ($-C\underline{H}_3$; a). 13 C NMR chemical shifts (126 MHz, CDCl₃, 25 °C): δ 170.86 $(-\underline{C}OO-)$, 68.28 $(-\underline{C}H_2O-)$, 37.90 $(-\underline{C}H_2CO-)$, 30.29 $(-\underline{C}H_2-)$, 26.17 $(-\underline{C}H(CH_3)-)$, and 20.98 $(-\underline{C}H_3)$.

Bifunctional telechelic poly(β -methyl- δ -valerolactone) (P β M δ VL) was synthesized through ROP of β M δ VL with 1,4-benzenedimethanol (BDM) as an initiator and diphenyl phosphate (DPP) as a catalyst. ^{33,36,37} To target a molar mass of 70 kDa with an assumed conversion efficiency of 85%, 0.155 g of BDM was dissolved in 78.62 g of β M δ VL in a 500 mL pressure vessel in a nitrogen atmosphere glovebox, followed by the addition of 0.196 g of DPP. The pressure vessel was sealed, and polymerization was continued at room temperature with stirring for 18 h. The reaction mixture was dissolved in DCM, and the solution was slowly added to an excess volume of cold MeOH to precipitate P β M δ VL; this purification step was performed three times. Purified P β M δ VL was dried in a fume hood overnight and further dried under vacuum for 3 days. P β M δ VL

was characterized with ^{1}H NMR, ^{13}C NMR, and size-exclusion chromatography (SEC). ^{1}H NMR chemical shifts (400 MHz, CDCl₃, 25 °C): δ 2.32 ($-\text{C}\underline{\text{H}}_2\text{CO}$), 1.71 and 1.53 ($-\text{C}\underline{\text{H}}_2-$), 4.13 ($-\text{C}\underline{\text{H}}_2\text{O}-$), 2.19 (the backbone methane proton $-\text{C}\underline{\text{H}}(\text{CH}_3)$), and 0.99 (the side-chain methyl protons $-\text{C}\underline{\text{H}}_3$). ^{13}C NMR chemical shifts (126 MHz, CDCl₃, 25 °C): δ 172.55 (-COO-), 62.21 ($-\text{CH}_2\text{O}-$), 41.42 ($-\text{C}\text{H}_2\text{CO}-$), 35.04 ($-\text{C}\text{H}_2-$), 27.35 ($-\text{C}\text{H}(\text{CH}_3)-$), and 19.47 ($-\text{C}\text{H}_3$). Number average molar mass ($M_{\rm n}$) and dispersity (\oplus) were determined by SEC analysis.

Synthesis of Poly(ε -caprolactone)-co-poly(β -methyl- δ -valerolactone)-co-poly(ε -caprolactone) (PCL-P β M δ VL-PCL) Triblock **Polymers.** Triblock PCL-P β M δ VL-PCL polymers were synthesized by ROP of ε -caprolactone using bifunctional telechelic P β M δ VL as a macroinitiator. 38,39 In a nitrogen atmosphere glovebox, PetaM δ VL was dissolved in anhydrous toluene at a concentration of 0.4 g/mL in a pressure vessel at 130 °C. After the solution was cooled to room temperature, caprolactone and the catalyst (Sn(Oct)₂) were added. The amount of caprolactone was calculated according to the desired molar mass and an assumed conversion efficiency of 85%; the weight ratio of Sn(Oct), to caprolactone was 1:1000. The pressure vessel was sealed and placed in an oil bath at 110 °C; the reaction was continued for 4 h under stirring. The reaction mixture was dissolved in DCM, and the solution was slowly added to an excess volume of cold MeOH to precipitate the polymer; this step was repeated three times. Purified triblock polymers were dried in a fume hood overnight and further dried under vacuum for 3 days. The products were characterized with ¹H NMR, ¹³C NMR, and SEC. ¹H NMR chemical shifts (400 MHz, CDCl₃, 25 °C: δ 4.13–4.11 (-CH₂OH), 2.35–2.09 (-CH₂CO- and $-C\underline{H}(CH_3)$), 1.67–1.39 ($-C\underline{H}_2$ –), and 0.99 ($-C\underline{H}_3$)). ¹³C NMR chemical shifts (126 MHz, CDCl₃, 25 °C): δ 173.48 (-COO-), 172.55 ($-\underline{C}OO-$), 64.10 ($-\underline{C}H_2O-$), 62.21 ($-\underline{C}H_2O-$), 41.42 $(-\underline{C}H_2CO-)$, 35.04 $(-\underline{C}H_2-)$, 34.08 $(-\underline{C}H_2CO-)$, 28.31 $(-\underline{C}H_2-)$, 27.35 $(-\underline{C}H(CH_3)-)$, 25.46 $(-\underline{C}H_2-)$, 24.54 $(-\underline{C}H_2-)$, and 19.47 $(-\underline{C}H_3)$. M_n and D of each polymer were determined by SEC analysis. The fraction of PCL end blocks in each triblock polymer (F_{CL}) was calculated by comparing the molar masses of P β M δ VL and the triblock polymer.

NMR and SEC Analyses. Polymers were dissolved in deuterated chloroform (CDCl₃), and NMR analyses (¹H and ¹³C) were performed using a 400 MHz Bruker Advance III NMR spectrometer to characterize their chemical structures. NMR experiments were conducted at 25 °C, and data analysis was performed using the CDCl₃ peak as a reference. M_n and D of each polymer were determined by SEC analysis with a calibration curve produced from narrowly dispersed polystyrene and Wyatt ASTRA Software. SEC was performed with three Phenomenex Phenogel-5 columns at 25 °C, and THF was used as the mobile phase at a flow rate of 1 mL/min.

Thermal Analysis. Differential scanning calorimetry (DSC) was performed on a TA Discovery Series (Q1000) DSC instrument. In the first cycle, samples were heated to 100 °C and held there for 2 min, and then cooled to -80 °C and held there for 2 min; in the second cycle, samples were heated from -80 to 100 °C. A rate of 2 °C/min was used for both heating and cooling. The thermogram of the second cycle was used to determine the melting temperature and melting enthalpy of each triblock polymer. Melting enthalpy of PCL end blocks in each triblock polymer was determined by dividing the melting enthalpy of the triblock polymer by the fraction of PCL ($F_{\rm CL}$). Crystallinity of PCL end blocks was determined by comparing the melting enthalpy to that of 100% crystalline PCL (139.5 J/g). 40,41

Fabrication of Polymer Films. Polymer films approximately 0.2 mm thick were fabricated by hot-pressing. Each material was sandwiched between two Teflon sheets and placed in a preheated (60 °C) Carver 4386 hot-press, pressed at 350 kPa and 60 °C for 5 min, removed from the press, and cooled to room temperature.

Characterization of Mechanical Properties. A dog bone-shaped die (14 mm gauge length; 3.4 mm width) was used to cut specimens from hot-pressed polymer films. The thickness of each specimen was measured with a caliper. Uniaxial extension and tensile hysteresis tests were performed with a strain rate of 10 mm/min on a Shimadzu AGS-X tensile tester. Uniaxial extension tests revealed

tensile strength, strain to failure, and Young's modulus (determined in the low strain region (0-5%)) of each stress—strain curve. ⁴² Tensile hysteresis tests were performed with a maximal strain of 50% for 20 cycles to reveal hysteresis loss and residual strain. Hysteresis loss was determined from the area between loading and unloading stress—strain curves in each cycle, and the residual strain was determined by the strain when the unloading curve reached zero stress. ⁴³

Tensile set was measured on a TestResources Q100 Tensile Tester following ASTM standard D412-16.⁴⁴ Specimens were stretched to 50% strain within 15 s, held there for 10 min, and retracted at a rate of 10 mm/min. After the grip returned to its starting position, the specimen was removed from the apparatus, and specimen length was measured with a caliper immediately and every 10 min afterward. The remaining strain (tensile set) at various time points was calculated by dividing the change in the specimen length (with respect to the initial length) by the initial length.

Contact Angle Measurement. Water contact angle of polymer samples was measured using the sessile drop method. Deionized water (3 μ L) was placed on each sample, and the contact angle was measured on a Kyowa DM-CE1 contact angle meter with FAMAS software.

Encapsulation of Lysozyme in PCL-PβMδVL-PCL. Lysozyme was encapsulated in PCL_{15} -PβMδVL-PCL₁₅ through melt blending in a twin-screw extruder (Microcompounder, DACA Instruments) as previously reported. ⁴⁵ The polymer was first hot-pressed (350 kPa; 60 °C) to a 0.2 mm thick film, which was then rolled with lysozyme powder and fed into the extruder (the polymer to lysozyme weight ratio was 4:1). Melt blending was performed at 60 °C under a N_2 atmosphere for 10 min, with rotation speed of the twin-screw maintained at 100 rpm. The melt blended sample was further hot-pressed to a 0.2 mm thick film at 60 °C.

Distribution of lysozyme particles in the film was examined on an Olympus IX70 inverted microscope with a 10× objective (0.25 NA). To evaluate whether multiple processing procedures at 60 °C affected lysozyme activity, 2 g of the film was dissolved in 20 mL of DCM, followed by extraction of lysozyme with 10 mL of water and lyophilization. The ratio of the weight of the extracted lysozyme to 2 g was calculated to determine the actual lysozyme loading content. Activity of the extracted lysozyme was examined using a lysozyme activity assay kit according to the manufacturer's instructions (Thermo Fisher Scientific). Activity of pristine lysozyme and DCM-treated lysozyme was prepared by dispersing pristine lysozyme in DCM, followed by extraction with water and lyophilization.

Printing Process. Printing of PCL_{15} - $P\beta M\delta VL$ - PCL_{15} at 60 °C was performed on a CELLINK's BIO-X 3D printing instrument with a thermoplastic printhead setup. A hand-shaped pattern was designed in SolidWorks. A polymer film was fed into the heating chamber of the printhead and heated at 60 °C for 10 min, and the polymer melt was printed with a speed of 0.5 mm/min under a pressure of 200 kPa.

Assessment of Material Cytocompatibility. To evaluate material cytocompatibility, specimens were cut from hot-pressed films using a 6 mm biopsy punch, mounted on the bottom of 96-well plates via a thin layer of autoclaved vacuum grease, incubated with 500 U/mL penicillin-streptomycin solution for 2 h for sterilization, and washed with phosphate buffer saline (PBS) three times. Commercial tissue culture polystyrene (TCPS) was used as a control. Fibroblasts (NIH 3T3) were plated at a density of 15537 cells/cm² and cultured in Dulbecco's modified Eagle's medium (DMEM) supplemented with 10% FBS and 100 U/mL penicillin-streptomycin. At 24 h postseeding, cell viability was evaluated with Alamar Blue assay according to the manufacturer's instructions. Briefly, Alamar Blue reagent (10% v/v) was added to each well and incubated for 4 h, followed by measuring the fluorescence intensity of the medium (excitation at 560 nm; emission at 590 nm) on a BioTek Cytation 3 plate reader. 46 To evaluate cell viability at longer time, fibroblasts were seeded at a density of 3107 cells/cm², and Alamar Blue assay was performed after 1, 3, and 5 days. All experiments were conducted in triplicate.

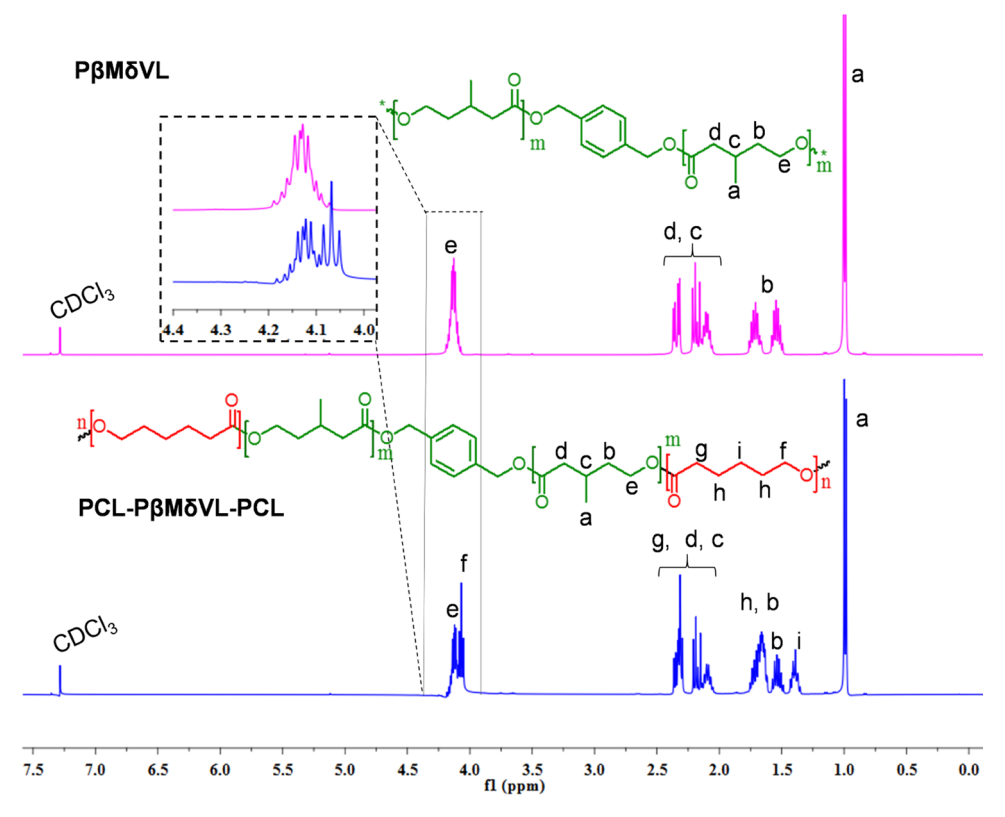


Figure 1. ¹H NMR spectra of PβMδVL and PCL₃₀-PβMδVL-PCL₃₀ dissolved in CDCl₃.

Table 1. Compositional and Physicochemical Properties of Synthesized Polymers^a

polymers	$^{1}M_{\rm n}~({\rm kDa})$	1 Đ	$^{2}F_{\mathrm{CL}}$	$^3T_{\rm m}$ (°C)	melting enthalpy (J/g)	⁴ crystallinity of PCL end blocks (%)
P β M δ VL	62.72	1.01	0	N/A	N/A	N/A
PCL_{10} - $P\beta M\delta VL-PCL_{10}$	82.31	1.13	0.24	52.2	13.99	41.78
PCL_{15} - $P\beta M\delta VL-PCL_{15}$	90.64	1.12	0.30	52.9	18.92	45.20
PCL_{20} - $P\beta M\delta VL-PCL_{20}$	94.92	1.14	0.34	53.4	21.88	46.13
PCL_{30} - $P\beta M\delta VL$ - PCL_{30}	100.03	1.23	0.37	54.3	28.64	55.48

 $^{^{}a1}M_{\rm n}$ = number average molar mass and Θ = dispersity, both determined by SEC; $^2F_{\rm CL}$ = fraction of PCL, calculated by comparing molar masses of P β M δ VL and each triblock polymer (e.g., $F_{\rm CL}$ for PCL $_{10}$ -P β M δ VL-PCL $_{10}$ = [(82.31-62.72)/82.31] = 0.24); and $^3T_{\rm m}$ = melting temperature, determined by differential scanning calorimetry (DSC). 4 Calculated by comparing the melting enthalpy of PCL end blocks (determined by dividing the melting enthalpy of each triblock polymer by $F_{\rm CL}$) with that of 100% crystalline PCL (139.5 J/g).

Scheme 1. Synthesis of PCL-P β M δ VL-PCL Triblock Polymers through a Two-Step Ring-Opening Polymerization Method

Material cytocompatibility was further examined using live—dead cell staining. Fibroblasts were plated at a density of 3107 cells/cm^2 on polymer films and cultured for 1 or 5 days, followed by staining with ethidium homodimer and calcein AM (0.1% v/v) for 30 min. Polymer specimens were placed on a glass slide with the cell side facing down, and fluorescence images were acquired on an Olympus IX70 inverted fluorescence microscope.

Degradation Kinetics. Specimens were cut from hot-pressed, 0.2 mm thick polymer films using an 8 mm biopsy punch, and the initial weight of each specimen was recorded. Each specimen was placed in a 15 mL Falcon tube containing 5 mL of sterilized PBS or 2000 U/mL lipase (*T. lanuginosus*) solution prepared in PBS and incubated at 37 °C. The solution in each tube was replaced with a fresh solution, weekly. At various time points, specimens were washed, dried, and

weighed. Weight loss was calculated by subtracting the final weight from the initial weight.

Statistical Analyses. Measurement of mechanical properties, lysozyme activity after encapsulation, cytocompatibility, and polymer degradation kinetics were performed in triplicate. Results are reported as the mean \pm std dev. Welch's one-way ANOVA with Dunnett's multiple comparison posthoc test or two-way ANOVA with Tukey's multiple comparison posthoc test was performed, as indicated in figure legends. Statistical analyses were performed using GraphPad Prism 9.0.

RESULTS AND DISCUSSION

Synthesis of $\beta M\delta VL$, $P\beta M\delta VL$, and $PCL-P\beta M\delta VL-PCL$.

The lactone monomer $\beta M\delta VL$ was successfully synthesized from 3-methyl-1,5-pentanediol, as confirmed by 1H and ^{13}C NMR analyses (Figures S1 and S2). P $\beta M\delta VL$ was successfully synthesized via ROP of $\beta M\delta VL$, as confirmed by 1H and ^{13}C NMR analyses (Figures 1 and S3). The single-resonance peak at 4.13 ppm instead of two methylene proton peaks at 4.23 and 4.08 ppm in the 1H NMR spectrum confirmed lactone ringopening. SEC analysis of the P $\beta M\delta VL$ revealed a M_n of 62.72 kDa (close to the targeted molar mass of 70 kDa) and a narrow dispersity of 1.01 (Table 1).

PCL-PβMδVL-PCL triblock polymers were synthesized via ROP of the commercially available caprolactone monomer with the telechelic PβMδVL diol as a macroinitiator (Scheme 1). Four compositionally different triblock polymers were synthesized by tuning the molar mass of PCL end blocks: PCL₁₀-PβMδVL-PCL₁₀, PCL₁₅-PβMδVL-PCL₁₅, PCL₂₀-PβMδVL-PCL₂₀, and PCL₃₀-PβMδVL-PCL₃₀ (the subscripted numbers adjacent to PCL blocks represent the targeted molar masses in kDa). Successful synthesis of triblock polymers was confirmed by 1 H NMR, 13 C NMR, and SEC analyses.

Chemical shifts corresponding to $P\beta M\delta VL$ and PCL were observed in NMR spectra (Figures 1, S3, and S4). SEC chromatograms of the products shifted toward shorter retention times (corresponding to larger molar masses) as compared with that of $P\beta M\delta VL$, suggesting that PCL was linked to $P\beta M\delta VL$ (Figure 2). Furthermore, triblock polymer syntheses targeting longer PCL end blocks yielded shorter retention times than those targeting shorter PCL end blocks, suggesting that compositionally different triblock polymers were synthesized as designed (Figure 2). The molar mass and

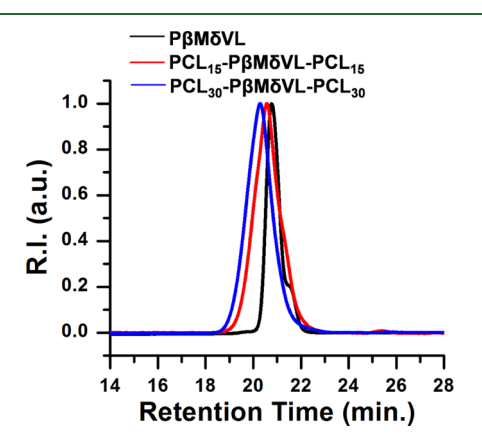


Figure 2. SEC analysis for synthesized polymers. The retention times of PCL₁₅-P β M δ VL-PCL₁₅ and PCL₃₀-P β M δ VL-PCL₃₀ were shorter than that of P β M δ VL, suggesting successful synthesis of triblock polymers.

dispersity of each triblock polymer were determined by SEC analysis and are shown in Table 1.

Thermal Properties of P β M δ VL and PCL-P β M δ VL-PCL. DSC analysis of P β M δ VL revealed a glass-transition temperature ($T_{\rm g}$) of -51 °C with no melting peak (Figure 3),

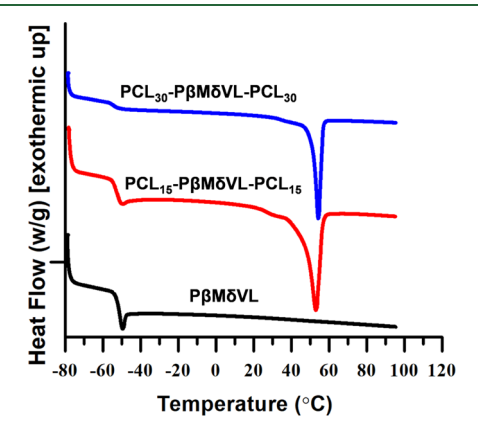


Figure 3. DSC thermograms of PβMδVL and PCL-PβMδVL-PCL. PβMδVL has a glass transition at -51 °C and no melting peak; PCL-PβMδVL-PCL polymers have a glass transition at -51 °C and a melting peak below 55 °C.

consistent with previous reports.³³ DSC analysis of PCL-P β M δ VL-PCL triblock polymers revealed both a glass transition at the same $T_{\rm g}$ of P β M δ VL and a melting peak in the range 52–55 °C (Figure 3).

The low $T_{\rm g}$ of the amorphous P\$\beta M\delta VL\$ midblock allows it to be in the rubbery state at physiological temperature, providing elastomeric properties for PCL-P\$\beta M\delta VL-PCL\$ polymers. The melting peak observed for PCL-P\$\beta M\delta VL-PCL\$ polymers suggested that PCL end blocks were crystalline or semicrystalline, serving as physical junctions to provide mechanical strength and modulus. The melting temperature (\$T_{\mu}\$) of triblock polymers slightly increased with the PCL block length, but all PCL-P\$\beta M\delta VL-PCL\$ polymers had a \$T_{\mu}\$ below 55 °C (Table 1).

Crystallinity (X_c) of PCL end blocks in each triblock polymer was determined by the ratio of the melting enthalpy of PCL end blocks (calculated from melting enthalpy and composition of the triblock polymer) to 139.50 J/g, which is the melting enthalpy of 100% crystalline PCL.41 The crystallinity of PCL end blocks was 41.78, 45.20, 46.13, and 55.48% for PCL_{10} - $P\beta M\delta VL$ - PCL_{10} , PCL_{15} - $P\beta M\delta VL$ - PCL_{15} , PCL_{20} - $P\beta M\delta VL$ - PCL_{20} , and PCL_{30} - $P\beta M\delta VL$ - PCL_{30} , respectively (Table 1). Crystallinity of PCL end blocks increased slightly with PCL block length, probably because the crystalline structure of PCL segments adjacent to the amorphous P β M δ VL midblock was disrupted and the percentage of disrupted segments decreased with increasing PCL block length. The increase in crystallinity of PCL end blocks with increasing block length may explain the slight increase in the melting temperature of PCL-P β M δ VL-PCL polymers with PCL end block length.4

Mechanical Properties of PCL-PβMδVL-PCL. Young's modulus, ultimate tensile strength, and strain to failure of PCL-PβMδVL-PCL polymers were determined from uniaxial stress–strain curves (Figures 4a and S5a; Table 2). Young's modulus determined from the low strain region (0-5%) ranged from 12 to 49 MPa and increased with PCL end block length.

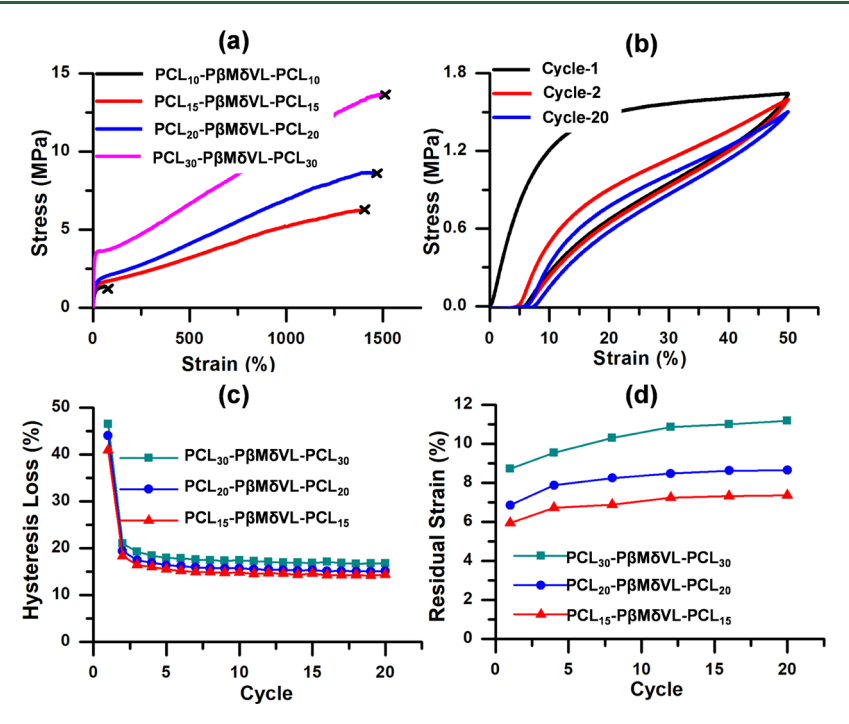


Figure 4. Uniaxial extension and cyclic tensile tests for PCL-P β M δ VL-PCL polymers. (a) Representative stress—strain curves of uniaxial extension tests. (b) Representative stress—strain curves of cyclic tensile tests for PCL₁₅-P β M δ VL-PCL₁₅. (c) Hysteresis energy loss determined from cyclic tensile tests. (d) Residual strain in cyclic tensile tests. All tests were performed with a strain rate of 10 mm/min.

Table 2. Mechanical Properties of PCL-P β M δ VL-PCL Polymers^a

polymers	¹ E (MPa)	² residual strain (%)	ultimate strength (MPa)	strain to failure (%)
PCL_{10} - $P\beta M\delta VL$ - PCL_{10}	12.78 ± 2.05	N/A*	1.39 ± 0.4	66 ± 9.12
PCL_{15} - $P\beta M\delta VL$ - PCL_{15}	14.76 ± 1.39	7.37 ± 0.42	6.24 ± 0.68	1394 ± 20.98
PCL_{20} - $P\beta M\delta VL$ - PCL_{20}	16.78 ± 0.91	8.65 ±0.49	8.59 ± 0.51	1458 ± 28.37
PCL_{30} - $P\beta M\delta VL$ - PCL_{30}	48.52 ± 7.26	11.18 ± 0.78	13.60 ± 2.17	1502 ± 41.25

 ^{a1}E = Young's modulus and 2 residual strain at the 20th cycle. *PCL $_{10}$ -P β M δ VL-PCL $_{10}$ failed during the second cycle. n = 3. Results are reported as the mean \pm std dev.

Ultimate tensile strength also increased with PCL end block length from approximately 1.4 MPa for PCL₁₀-P β M δ VL-PCL₁₀ to 13.6 MPa for PCL₃₀-P β M δ VL-PCL₃₀. Strain to failure was greater than 1000% for PCL₁₅-P β M δ VL-PCL₁₅, PCL₂₀-P β M δ VL-PCL₂₀, and PCL₃₀-P β M δ VL-PCL₃₀, suggesting that these polymers are highly stretchable. PCL₁₀-P β M δ VL-PCL₁₀ showed much lower ultimate tensile strength than the other three triblock polymers, and its strain to failure was only 66%, suggesting that the junctions formed from 10 kDa PCL end blocks are not strong enough to allow extensive stretching.

Tensile hysteresis tests for PCL_{15} - $P\beta M\delta VL$ - PCL_{15} , PCL_{20} - $P\beta M\delta VL$ - PCL_{20} , and PCL_{30} - $P\beta M\delta VL$ - PCL_{30} revealed that hysteresis energy loss during the first cycle was relatively large (42–47%) but became significantly smaller for all subsequent cycles (15–18% at cycle 5; 14–17% at cycle 20), suggesting that these polymers are elastomers (Figure 4b,c). The increase in residual strain was most significant in the first cycle, and only a minor increase was observed in each subsequent cycle (Figure 4d). Among the three elastomers, PCL_{15} - $P\beta M\delta VL$ - PCL_{15} exhibited the least hysteresis energy loss (15.5% at cycle 5 and 14% at cycle 20) and residual strain (6.7% at cycle 5 and 7.37% at cycle 20), suggesting that shorter PCL end blocks endow better elastomeric properties provided they are long enough to form strong junctions to allow extensive stretching.

Tensile set (defined as remaining strain after a specimen has been stretched and allowed to retract in a specified manner) of PCL_{15} - $P\beta M\delta VL$ - PCL_{15} was measured according to ASTM standard D412-16 (Figure S5b). As Specimens were stretched to 50% strain within 15 s, held there for 10 min, and retracted at a rate of 10 mm/min. Tensile set was 3.4% (i.e., strain recovery was 96.60%) immediately following the tester grip returning to its starting position. After 10 min, tensile set was 1.76% (i.e., strain recovery was 98.24%), and complete recovery was observed after 40 min. These results further confirm that PCL- $P\beta M\delta VL$ -PCL polymers are elastomeric.

Cytocompatibility of PCL-PβMδVL-PCL Elastomers. Alamar Blue assay performed for fibroblasts cultured on films of the three PCL-PβMδVL-PCL elastomers for 24 h revealed similar cell viability to that on the positive control of commercial TCPS (Figure 5a). Alamar Blue assay was further performed for fibroblasts cultured on PCL₁₅-PβMδVL-PCL₁₅ films for up to 5 days, and cell viability evaluated at each time point was similar to that on the TCPS control (Figure 5b). In addition, the Alamar Blue fluorescence signal increased by approximately 1.6 times between days 1 and 5 on PCL₁₅-PβMδVL-PCL₁₅ films, suggesting that the material supported cell proliferation. Cytocompatibility of PCL-PβMδVL-PCL elastomers was further confirmed by live—dead cell staining. A few dead cells were observed on either PCL-PβMδVL-PCL

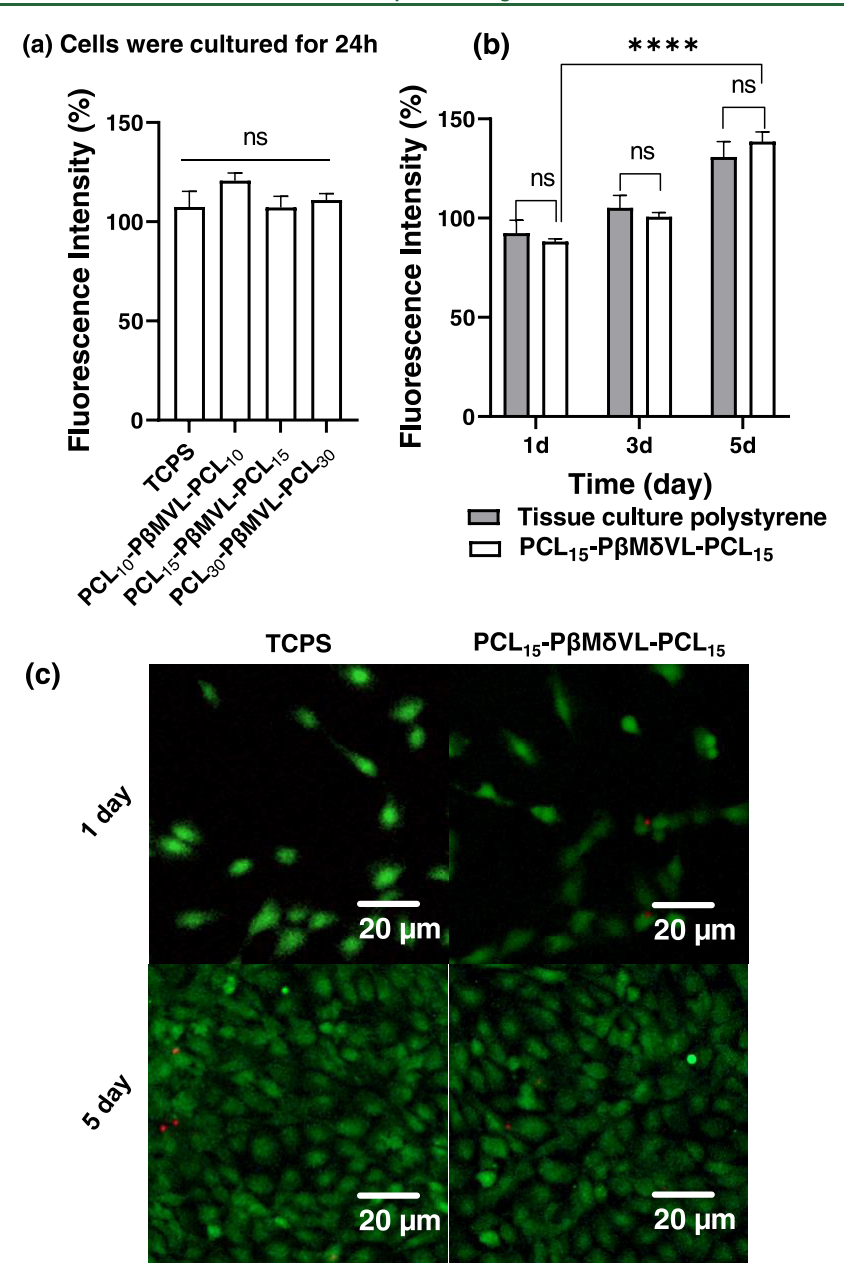


Figure 5. Evaluation of cytocompatibility of PCL-PβMδVL-PCL elastomers. Commercial tissue culture polystyrene (TCPS) was used as a control. (a) Alamar Blue assay for 3T3 fibroblasts seeded at 15537 cells/cm² on triblock elastomers and cultured for 24 h. (b) Alamar Blue assay for 3T3 fibroblasts seeded at 3107 cells/cm² on PCL₁₅-PβMδVL-PCL₁₅ and cultured for 5 days. (c) Representative images of live—dead staining for 3T3 fibroblasts seeded at 3107 cells/cm² on PCL₁₅-PβMδVL-PCL₁₅ and cultured for 1 and 5 days. Results are reported as the mean \pm std dev. Statistical analysis was performed using Welch's one-way ANOVA with Dunnett's multiple comparison posthoc test for (a) and two-way ANOVA with Tukey's multiple comparison posthoc test for (b), ns = not significant (*p*-value > 0.05), *****p*-value < 0.0001, and *n* = 3.

polymer films or TCPS (Figure 5c). These results suggest that PCL-P β M δ VL-PCL elastomers are as cytocompatible as commercial TCPS.

Printing of PCL-PβMδVL-PCL Elastomers. The thermoplastic nature of PCL-PβMδVL-PCL elastomers and their relatively low melting temperatures (below 55 °C) make it easy to process these materials into desired shapes and structures. We demonstrated that they could be readily printed by commonly used fused deposition modeling (FDM) technology on a BIO-X 3D printer equipped with a thermoplastic head. PCL₁₅-PβMδVL-PCL₁₅ was fed into the printer head and heated to 60 °C, and the polymer melt was printed with a

pressure of 200 kPa to form a hand-shaped structure shown in Figure 6.

Protein Encapsulation in PCL-PβMδVL-PCL Elastomers. Lysozyme, which has a denaturation temperature of 75 $^{\circ}$ C, 49 was chosen as a model bioactive agent. Lysozyme was encapsulated in PCL₁₅-PβMδVL-PCL₁₅ via melt blending at 60 $^{\circ}$ C in a twin-screw extruder, and the melt blended product was further hot-pressed to 0.2 mm thick films at 60 $^{\circ}$ C under 350 kPa pressure. Examination of these films with optical microscopy revealed that lysozyme particles were uniformly distributed throughout each specimen, whereas the distribution of lysozyme particles encapsulated in PCL₁₅-PβMδVL-PCL₁₅ via solvent casting was not uniform (Figure S6). The



Figure 6. Thermoplastic PCL_{15} - $P\beta M\delta VL$ - PCL_{15} was printed to a hand-shaped structure through fused deposition modeling (FDM) at 60 °C.

lysozyme loading content was 18.25%. Uniaxial tensile tests showed that Young's modulus of PCL_{15} - $P\beta M\delta VL-PCL_{15}$ containing lysozyme was 14.68 MPa (Figure S7), similar to that of pristine polymer. Strain to failure was 959%, and ultimate tensile strength was 5.46 MPa; both values were slightly lower than those for pristine polymer.

Activity of the lysozyme encapsulated in PCL_{15} - $P\beta M\delta VL-PCL_{15}$ films was examined to assess whether the double processing procedures at 60 °C (melt blending and hotpressing) damaged protein activity. To retrieve encapsulated lysozyme, the films were treated with DCM to dissolve the polymer, followed by extraction of lysozyme with water and lyophilization. Pristine lysozyme and DCM-treated lysozyme were evaluated as two controls. The activity of the lysozyme extracted from the films was slightly lower than that of pristine lysozyme (p-value = 0.12), but almost the same as that of DCM-treated lysozyme (p-value > 0.9999) (Figure 7). These results suggested that lysozyme slightly lost its activity when exposed to DCM, but the double processing procedures at 60 °C did not reduce its activity.

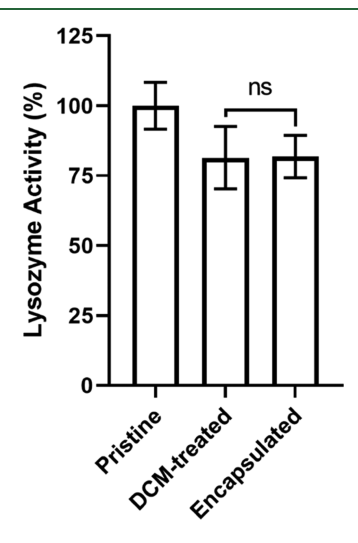


Figure 7. Activity of the lysozyme encapsulated in PCL₁₅-P β M δ VL-PCL₁₅ films through double heat processing at 60 °C (melt blending and hot-pressing) and extracted with DCM. Pristine lysozyme and DCM-treated lysozyme were evaluated as controls. Results are reported as the mean \pm std. dev. Statistical analysis was performed using Welch's one-way ANOVA with Dunnett's multiple comparison posthoc test, ns= not significant (p-value > 0.9999), and p = 3.

Encapsulation of bioactive agents in a material is often required for biomedical applications. These bioactive agents are often proteins, which could be affected by material processing when performed at high temperatures or with organic solvents. Thermoplastic polymers can be processed at an elevated temperature (such as $T_{\rm m}$ for semicrystalline polymers) while under pressure or via solvent casting. In general, solvent casting is not ideal because proteins could denature in an organic solvent, resulting in loss of structure and activity, and residual solvent could be cytotoxic. Thermal processing does not leave toxic substances behind but many materials require a high processing temperature, which could also lead to protein denaturation. In this work, we demonstrated that lysozyme, which has a denaturation temperature of 75 °C, can be uniformly encapsulated in PCL-P β M δ VL-PCL films using a double thermal processing method at 60 °C (melt blending and hot-pressing) without any loss of its bioactivity. Therefore, PCL-PβMδVL-PCL elastomers could be readily processed into products encapsulating bioactive agents that retain activity at 60 °C, even though it remains challenging to encapsulate sensitive agents that lose bioactivity at or above 60 °C.

Water Contact Angle of PCL-PβMδVL-PCL. Water contact angles (CAs) of PCL₁₅-PβMδVL-PCL₁₅, PβMδVL, and PCL₄₅ were 104, 96, and 113°, respectively (Figure S8), suggesting that PβMδVL is less hydrophobic than PCL₄₅ and that both PβMδVL and PCL blocks coexist on the surface of PCL₁₅-PβMδVL-PCL₁₅. The CA of PCL₁₅-PβMδVL-PCL₁₅ films encapsulating lysozyme was 81° (Figure S8), suggesting that lysozyme was present on the surface of these films.

Degradation of PCL-PβMδVL-PCL. PCL-PβMδVL-PCL elastomers are polyesters and are expected to be hydrolyzable. Degradation of PCL₁₅-PβMδVL-PCL₁₅ was examined *in vitro* by incubating polymer specimens in PBS and in a solution of lipase (T. lanuginosus; 2000 U/mL) at 37 °C for up to 8 weeks. In PBS, mass loss was negligible at 1 week and increased almost linearly between 1 and 8 weeks to approximately 8% (Figure 8). In lipase solution, polymer degradation was significantly accelerated and mass loss was 63% at 8 weeks, consistent with previous reports on lipase accelerated hydrolysis of ester bonds (Figure 8). These results confirm

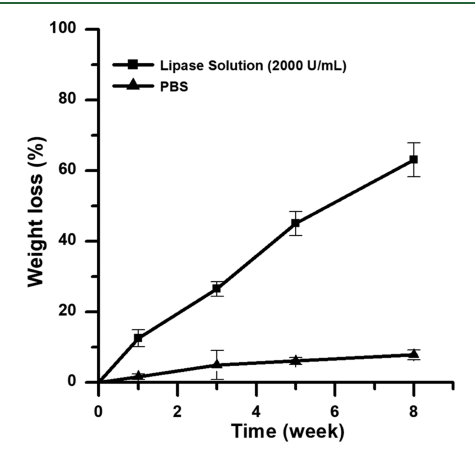


Figure 8. Weight loss profiles of PCL₁₅-PβMδVL-PCL₁₅ incubated in PBS and a lipase solution at 37 °C for 8 weeks. Results are reported as average of three independent experiments (n = 3) and error bars represent \pm std. dev.

that PCL-P β M δ VL-PCL elastomers are hydrolyzable, and their degradation is accelerated in the presence of lipase.

CONCLUSIONS

Thermoplastic PCL-P β M δ VL-PCL triblock polymers were successfully synthesized. The triblock polymers exhibited elastomeric properties when the P β M δ VL midblock was 62.7 kDa, and the two PCL end blocks were in the range of 14.0-18.7 kDa. These materials have strain to failure values greater than 1000%. Tensile set measurements according to an ASTM standard revealed a 98.24% strain recovery 10 min after the force was removed and complete strain recovery 40 min after the force was removed. The amorphous P β M δ VL midblock displayed a $T_{\rm g}$ of -51 °C, and PCL end blocks were semicrystalline with a $T_{\rm m}$ in the range of 52-55 °C. Due to their thermoplastic nature and low melting temperatures, these elastomers were readily processable using printing, extrusion, or hot-pressing at 60 °C, and lysozyme encapsulated in PCL- $P\beta M\delta VL$ -PCL elastomers during processing did not lose bioactivity. PCL-P β M δ VL-PCL polymers were as cytocompatible as commercial tissue culture polystyrene in supporting cell viability and cell growth, and they were degradable in aqueous environments through hydrolysis. These degradable, cytocompatible, elastomeric, and thermoplastic materials are potentially amenable to 3D printing at 60 °C and may find many applications in the biomedical field, such as medical devices and tissue engineering scaffolds.

ASSOCIATED CONTENT

Supporting Information

The Supporting Information is available free of charge at https://pubs.acs.org/doi/10.1021/acs.biomac.1c01197.

Supporting information contains ^{1}H and ^{13}C NMR; tensile test; microscopic images of a lysozyme-encapsulated PCL-P β M δ VL-PCL film; and water contact angle (PDF)

AUTHOR INFORMATION

Corresponding Author

Wei Shen — Department of Biomedical Engineering, University of Minnesota, Minneapolis, Minnesota 55455, United States; orcid.org/0000-0002-3143-3234; Phone: +1 612 624 3771; Email: shenx104@umn.edu; Fax: +1 612 626 6583

Authors

Sudipta Panja – Department of Biomedical Engineering, University of Minnesota, Minneapolis, Minnesota 55455, United States; orcid.org/0000-0001-5692-450X

Allison Siehr – Department of Biomedical Engineering, University of Minnesota, Minneapolis, Minnesota 55455, United States; Occid.org/0000-0002-8186-0007

Anasuya Sahoo – Department of Pharmaceutics, University of Minnesota, Minneapolis, Minnesota 55455, United States

Ronald A. Siegel — Department of Biomedical Engineering, University of Minnesota, Minneapolis, Minnesota 55455, United States; Department of Pharmaceutics, University of Minnesota, Minneapolis, Minnesota 55455, United States; orcid.org/0000-0002-9591-1282

Complete contact information is available at: https://pubs.acs.org/10.1021/acs.biomac.1c01197

Author Contributions

S.P.: lead author, designed and performed all experiments, except the tensile set experiment and extrusion molding, analyzed data, and wrote the manuscript; A.S.: performed the tensile set experiment, analyzed data, and wrote the manuscript; A.Sah.: performed extrusion molding and thermal analysis; R.A.S.: codesigned experiments, analyzed data, and edited the manuscript; W.S.: led the project, codesigned experiments, analyzed data, and wrote the manuscript. All authors have approved the final version of the manuscript.

Notes

The authors declare no competing financial interest.

ACKNOWLEDGMENTS

The authors thank Prof. Marc Hillmyer for the use of the Shimadzu AGS-X tensile tester and the equipment for SEC-MALLS, Prof. Victor Barocas for use of the TestResources 100Q Tensile Tester, Prof. Dave Wood for the use of the Carver 4386 hot-press, Prof. Angela Panoskaltsis-Mortari for the use of the CELLINK's BIO-X 3D printing instrument, and Prof. Chun Wang for the use of synthesis equipment. The authors thank Prof. Chun Wang for discussions. Melt blending was carried out in the College of Science and Engineering Polymer Characterization Facility, University of Minnesota, which has received capital equipment funding from the National Science Foundation through the UMN MRSEC under Award number DMR-2011401. NMR analyses were performed in the LeClaire-Dow instrumentation facility, which is supported by the Office of the Vice President of Research, College of Science and Engineering, and the Department of Chemistry at the University of Minnesota. The authors used the glovebox in the Minnesota Nanocenter, which is supported by the National Science Foundation through the National Nanotechnology Coordinated Infrastructure (NNCI) under Award number ECCS-2025124. This work was supported by the University of Minnesota Industrial Partnership for Research in Interfacial and Materials Engineering (IPRIME) and the Institute for Engineering in Medicine (IEM).

REFERENCES

- (1) Zhang, Y.; Ding, J.; Qi, B.; Tao, W.; Wang, J.; Zhao, C.; Peng, H.; Shi, J. Multifunctional Fibers to Shape Future Biomedical Devices. *Adv. Funct. Mater.* **2019**, 29, No. 1902834.
- (2) Caballero Aguilar, L. M.; Silva, S. M.; Moulton, S. E. Growth factor delivery: Defining the next generation platforms for tissue engineering. *J. Controlled Release* **2019**, *306*, 40–58.
- (3) Zhao, X.; Dong, R.; Guo, B.; Ma, P. X. Dopamine-Incorporated Dual Bioactive Electroactive Shape Memory Polyurethane Elastomers with Physiological Shape Recovery Temperature, High Stretchability, and Enhanced C2C12 Myogenic Differentiation. ACS Appl. Mater. Interfaces 2017, 9, 29595–29611.
- (4) Wang, Y.; Ameer, G. A.; Sheppard, B. J.; Langer, R. A tough Biodegradable Elastomer. *Nat. Biotechnol.* **2002**, *20*, 602–606.
- (5) Levental, I.; Georges, P. C.; Janmey, P. A. Soft Biological Materials and Their Impact on Cell Function. *Soft Matter* **2007**, *3*, 299–306
- (6) Wellman, S. M.; Eles, J. R.; Ludwig, K. A.; Seymour, J. P.; Michelson, N. J.; McFadden, W. E.; Vazquez, A. L.; Kozai, T. D. Y. A Materials Roadmap to Functional Neural Interface Design. *Adv. Funct. Mater.* **2018**, 28, No. 1701269.
- (7) Zhang, Z.; Ortiz, O.; Goyal, R.; Kohn, J. Biodegradable Polymers. In *Principles of Tissue Engineering*; Elsevier, 2014; pp 441–473.
- (8) Li, C.; Guo, C.; Fitzpatrick, V.; Ibrahim, A.; Zwierstra, M. J.; Hanna, P.; Lechtig, A.; Nazarian, A.; Lin, S. J.; Kaplan, D. L. Design of

- Biodegradable, Implantable Devices Towards Clinical Translation. *Nat. Rev. Mater* **2020**, *5*, 61–81.
- (9) Li, W. J.; Cooper, J. A., Jr; Mauck, R. L.; Tuan, R. S. Fabrication and Characterization of Six Electrospun Poly(alpha-hydroxy ester)-based Fibrous Scaffolds for Tissue Engineering Applications. *Acta Biomater.* **2006**, *2*, 377–385.
- (10) Yang, J.; Webb, A. R.; Ameer, G. A. Novel Citric Acid-Based Biodegradable Elastomers for Tissue Engineering. *Adv. Mater.* **2004**, *16*, 511–516.
- (11) Tran, R. T.; Yang, J.; Ameer, G. A. Citrate-Based Biomaterials and Their Applications in Regenerative Engineering. *Annu. Rev. Mater. Res.* **2015**, *45*, 277–310.
- (12) Jaafar, I. H.; Ammar, M. M.; Jedlicka, S. S.; Pearson, R. A.; Coulter, J. P. Spectroscopic Evaluation, Thermal, and Thermomechanical Characterization of Poly(glycerol-sebacate) with Variations in Curing Temperatures and Durations. *J. Mater. Sci.* **2010**, *45*, 2525–2529.
- (13) Coneski, P. N.; Fulmer, P. A.; Wynne, J. H. Thermal Polycondensation of Poly(diol citrate)s with Tethered Quaternary Ammonium Biocides. *RSC Adv.* **2012**, *2*, 12824–12834.
- (14) Ye, H.; Zhang, K.; Kai, D.; Li, Z.; Loh, X. J. Polyester Elastomers for Soft Tissue Engineering. *Chem. Soc. Rev.* **2018**, 47, 4545–4580.
- (15) Rai, R.; Tallawi, M.; Grigore, A.; Boccaccini, A. R. Synthesis, Properties and Biomedical Applications of Poly(glycerol sebacate) (PGS): A review. *Prog. Polym. Sci.* **2012**, *37*, 1051–1078.
- (16) Lee, L. Y.; Wu, S. C.; Fu, S. S.; Zeng, S. Y.; Leong, W. S.; Tan, L. P. Biodegradable Elastomer for Soft Tissue Engineering. *Eur. Polym. J.* **2009**, *45*, 3249–3256.
- (17) Chen, Q.; Liang, S.; Thouas, G. A. Elastomeric Biomaterials for Tissue Engineering. *Prog. Polym. Sci.* **2013**, *38*, 584–671.
- (18) Chapanian, R.; Tse, M. Y.; Pang, S. C.; Amsden, B. G. The role of oxidation and enzymatic hydrolysis on the in vivo degradation of trimethylene carbonate based photocrosslinkable elastomers. *Biomaterials* **2009**, *30*, 295–306.
- (19) Annabi, N.; Mithieux, S. M.; Camci-Unal, G.; Dokmeci, M. R.; Weiss, A. S.; Khademhosseini, A. Elastomeric Recombinant Proteinbased Biomaterials. *Biochem. Eng. J.* **2013**, *77*, 110–118.
- (20) Zhang, Y. N.; Avery, R. K.; Vallmajo-Martin, Q.; Assmann, A.; Vegh, A.; Memic, A.; Olsen, B. D.; Annabi, N.; Khademhosseini, A. A Highly Elastic and Rapidly Crosslinkable Elastin-Like Polypeptide-Based Hydrogel for Biomedical Applications. *Adv. Funct. Mater.* **2015**, 25, 4814–4826.
- (21) Welsh, E. R.; Tirrell, D. A. Engineering the extracellular matrix: a novel approach to polymeric biomaterials. I. Control of the physical properties of artificial protein matrices designed to support adhesion of vascular endothelial cells. *Biomacromolecules* **2000**, *1*, 23–30.
- (22) Annabi, N.; Zhang, Y. N.; Assmann, A.; Sani, E. S.; Cheng, G.; Lassaletta, A. D.; Vegh, A.; Dehghani, B.; Ruiz-Esparza, G. U.; Wang, X.; Gangadharan, S.; Weiss, A. S.; Khademhosseini, A. Engineering a highly elastic human protein-based sealant for surgical applications. *Sci. Transl. Med.* **2017**, *9*, No. eaai7466.
- (23) Guelcher, S. A. Biodegradable Polyurethanes: synthesis and applications in regenerative medicine. *Tissue Eng., Part B* **2008**, *14*, 3–17.
- (24) de Groot, J. H.; V, Rd.; Wildeboer, B. S.; Spaans, C. S.; J, A. Pennings, New Biomedical Polyurethane Ureas with High Tear Strengths. *Polym. Bull.* **1997**, 38, 211–218.
- (25) Grabow, N.; Schmohl, K.; Khosravi, A.; Philipp, M.; Scharfschwerdt, M.; Graf, B.; Stamm, C.; Haubold, A.; Schmitz, K. P.; Steinhoff, G. Mechanical and structural properties of a novel hybrid heart valve scaffold for tissue engineering. *Artif. Organs* **2004**, 28, 971–979.
- (26) Avella, M.; Martuscelli, E.; Raimo, M. Review Properties of Blends and Composites Based on Poly(3-hydroxy)butyrate (PHB) and Poly(3-hydroxybutyrate-hydroxyvalerate) (PHBV) Copolymers. *J. Mater. Sci.* **2000**, *35*, 523–545.
- (27) Lee, S. H.; Kim, B. S.; Kim, S. H.; Choi, S. W.; Jeong, S. I.; Kwon, I. K.; Kang, S. W.; Nikolovski, J.; Mooney, D. J.; Han, Y. K.;

- Kim, Y. H. Elastic biodegradable poly(glycolide-co-caprolactone) scaffold for tissue engineering. *J. Biomed. Mater. Res., Part A* **2003**, 66A, 29–37.
- (28) Matsumura, G.; Hibino, N.; Ikada, Y.; Kurosawa, H.; Shin'oka, T. Successful Application of Tissue Engineered Vascular Autografts: clinical experience. *Biomaterials* **2003**, *24*, 2303–2308.
- (29) Zaky, S. H.; Lee, K. W.; Gao, J.; Jensen, A.; Verdelis, K.; Wang, Y.; Almarza, A. J.; Sfeir, C. Poly (glycerol sebacate) elastomer supports bone regeneration by its mechanical properties being closer to osteoid tissue rather than to mature bone. *Acta Biomater.* **2017**, *54*, 95–106.
- (30) Matsumura, G.; Miyagawa-Tomita, S.; Shin'oka, T.; Ikada, Y.; Kurosawa, H. First evidence that bone marrow cells contribute to the construction of tissue-engineered vascular autografts in vivo. *Circulation* **2003**, *108*, 1729–1734.
- (31) Li, L.; Raghupathi, K.; Song, C.; Prasad, P.; Thayumanavan, S. Self-assembly of Random Copolymers. *Chem. Commun.* **2014**, *50*, 13417–13432.
- (32) Cohn, D.; Salomon, A. H. Designing Biodegradable Multiblock PCL/PLA Thermoplastic Elastomers. *Biomaterials* **2005**, *26*, 2297–2305
- (33) Xiong, M.; Schneiderman, D. K.; Bates, F. S.; Hillmyer, M. A.; Zhang, K. Scalable Production of Mechanically Tunable Block Polymers from Sugar. *Proc. Natl. Acad. Sci. U.S.A.* **2014**, *111*, 8357–8362.
- (34) Panja, S.; Saha, B.; Ghosh, S. K.; Chattopadhyay, S. synthesis of novel four armed PE-PCL grafted superparamagnetic and biocompatible nanoparticles. *Langmuir.* **2013**, *29*, 12530–12540.
- (35) Panja, S.; Maji, S.; Maiti, T. K.; Chattopadhyay, S. A Smart Magnetically Active Nanovehicle for on-Demand Targeted Drug Delivery: Where van der Waals Force Balances the Magnetic Interaction. ACS Appl. Mater. Interfaces 2015, 7, 24229–24241.
- (36) Brutman, J. P.; De Hoe, G. X.; Schneiderman, D. K.; Le, T. N.; Hillmyer, M. A. Renewable, Degradable, and Chemically Recyclable Cross-Linked Elastomers. *Ind. Eng. Chem. Res.* **2016**, *55*, 11097—11106
- (37) Batiste, D. C.; Meyersohn, M. S.; Watts, A.; Hillmyer, M. A. Efficient Polymerization of Methyl- ε -Caprolactone Mixtures to Access Sustainable Aliphatic Polyesters. *Macromolecules* **2020**, *53*, 1795–1808.
- (38) Panja, S.; Dey, G.; Bharti, R.; Mandal, P.; Mandal, M.; Chattopadhyay, S. Metal Ion Ornamented Ultrafast Light-Sensitive Nanogel for Potential in Vivo Cancer Therapy. *Chem. Mater.* **2016**, 28, 8598–8610.
- (39) Panja, S.; Dey, G.; Bharti, R.; Kumari, K.; Maiti, T. K.; Mandal, M.; Chattopadhyay, S. Tailor-Made Temperature-Sensitive Micelle for Targeted and On-Demand Release of Anticancer Drugs. *ACS Appl. Mater. Interfaces* **2016**, *8*, 12063–12074.
- (40) Köncke, U.; Zachmann, H. G.; Baltá-Calleja, F. J. New Aspects Concerning the Structure and Degree of Crystallinity in High-Pressure-Crystallized Poly(ethylene terephthalate). *Macromolecules* **1996**, 29, 6019–6022.
- (41) Schneiderman, D. K.; Hill, E. M.; Martello, M. T.; Hillmyer, M. A. Poly(lactide)-block-poly(ε -caprolactone-co- ε -decalactone)-block-poly(lactide) Copolymer Elastomers. *Polym. Chem.* **2015**, *6*, 3641–3651.
- (42) Du, Y.; Yu, M.; Ge, J.; Ma, P. X.; Chen, X.; Lei, B. Development of a Multifunctional Platform Based on Strong, Intrinsically Photoluminescent and Antimicrobial Silica-Poly(citrates)-Based Hybrid Biodegradable Elastomers for Bone Regeneration. *Adv. Funct. Mater.* **2015**, 25, 5016–5029.
- (43) De Hoe, G. X.; Zumstein, M. T.; Tiegs, B. J.; Brutman, J. P.; McNeill, K.; Sander, M.; Coates, G. W.; Hillmyer, M. A. Sustainable Polyester Elastomers from Lactones: Synthesis, Properties, and Enzymatic Hydrolyzability. J. Am. Chem. Soc. 2018, 140, 963–973.
- (44) ASTM D412-16. Standard Test Methods for Vulcanized Rubber and Thermoplastic Elastomers—Tension; ASTM International: Conshohocken, PA, 2015.

- (45) Kim, H.; Miura, Y.; Macosko, C. W. Graphene/Polyurethane Nanocomposites for Improved Gas Barrier and Electrical Conductivity. *Chem. Mater.* **2010**, *22*, 3441–3450.
- (46) Moghanizadeh-Ashkezari, M.; Shokrollahi, P.; Zandi, M.; Shokrolahi, F.; Daliri, M. J.; Kanavi, M. R.; Balagholi, S. Vitamin C Loaded Poly(urethane-urea)/ZnAl-LDH Aligned Scaffolds Increase Proliferation of Corneal Keratocytes and Up-Regulate Vimentin Secretion. ACS Appl. Mater. Interfaces 2019, 11, 35525–35539.
- (47) Qian, H.; Bei, J.; Wang, S. Synthesis, Characterization and Degradation of ABA Block Copolymer of L-Lactide and ε -Caprolactone. *Polym. Degrad. Stab.* **2000**, *68*, 423–429.
- (48) Guvendiren, M.; Molde, J.; Soares, R. M.; Kohn, J. Designing Biomaterials for 3D Printing. *ACS Biomater. Sci. Eng.* **2016**, *2*, 1679–1693.
- (49) Goyal, M. K.; Roy, I.; Amin, A.; Banerjee, U. C.; Bansal, A. K. Stabilization of Lysozyme by Benzyl Alcohol: surface tension and thermodynamic parameters. *J. Pharm. Sci.* **2010**, *99*, 4149–4161.
- (50) Li, S.; Liu, L.; Garreau, H.; Vert, M. Lipase-Catalyzed Biodegradation of Poly(E-caprolactone) Blended with Various Polylactide-Based Polymers. *Biomacromolecules* **2003**, *4*, 372–377.